RAL-TR-98-024

THE PERFORMANCE OF GAS MICROSTRIP AND GAS PIXEL DETECTORS FOR USE ON ISIS BEAM LINES - A MONTE CARLO STUDY

J E Bateman, N J Rhodes and R Stephenson

Rutherford Appleton Laboratory, Chilton, Didcot, OX11 0QX

5 November 1997

ABSTRACT

A monte carlo model has been developed to simulate the interaction of a slow neutron beam with gas microstrip detectors (GMSD) and other forms of gas detector. The model permits the exploration of the trade-off between spatial resolution and detection efficiency in detectors proposed for various applications on ISIS.

1. INTRODUCTION

Following the successful test of an imaging beam monitor based on a gas microstrip detector (GMSD) [1] it became clear that gas detectors based on this technology could offer an interesting performance package for applications on ISIS beam lines. Using ^{3}He with a quencher, good rate capability and time resolution are combined with low gamma sensitivity and the potential to realise spatial resolution of the order of 1mm. There is an inevitable trade-off between detection efficiency and spatial resolution which is set by the counter depth, the gas pressure and the electronic discriminator threshold. This trade-off is determined largely by the range of the products of the ^{3}He disintegration (a proton and a triton) and the optimum counter specification for any given application can be examined conveniently by a montecarlo model of the interaction of these particles with the detector gas.

The model has been used to evaluate the design parameters of the following applications:

1. A high resolution (<0.5mm), low efficiency beam monitor.
2. An imaging detector of ≈1mm spatial resolution and intermediate detection efficiency (≈30%) for the study of engineering samples in the ENGIN facility.
3. A gas pixel detector for neutron diffraction studies. This would have a pixel edge of 2.5mm and realise a detection efficiency approaching 50%.
4. An evaluation of the performance to be expected from a very high pressure (16 bar) gas microstrip detector.

Note that the detection efficiencies are given for an incident neutron energy of 0.08eV, equivalent to a wavelength of 1A.

2. THE MONTE CARLO MODEL

The model works by generating randomly oriented back-to-back paths for the recoil proton (570keV) and triton (200keV) within a cell of the GMSD and tracing the paths of the particles until they either stop in a cell or pass out of the detector volume. The energy deposit in each cell traversed is evaluated and stored in an array using the range energy data published in reference [2]. A separate array sums all cell hits which are defined when the energy deposit in a cell exceeds the preset electronic threshold (LLD) which is defined in terms of the equivalent energy deposit in units of MeV.

For each simulation 10^4 starts are made on the basic loop which corresponds to that number of neutrons interacting in the gas. The *interaction efficiency* is simply calculated from the total stopping power of the ^{3}He present multiplied by the cross-section at a neutron wavelength of 1A. The *trigger efficiency* is measured as the fraction of the "starts" which result in at least one hit in a cell. The *detection efficiency* is thus the product of the trigger efficiency and the interaction efficiency.

A file containing the selected LLD, the array of cell counts and the two efficiency values is saved to disk. Often there is more than one hit per interacting neutron. The

multiplicity is defined as the area of the cell count profile divided by the number of starts.

Unless otherwise stated the model simulates the point spread function (PSF) of the detector, which is the response of the system to an input delta function. The incident "neutrons" are all generated at the centre of the zero pixel but are allowed to interact throughout its depth as would be the case for real neutrons.

Provision is made for an arbitrary choice of detector geometry i.e. the depth (d) (along the beam), width (c) and height (h) of the detector cells. Similarly an arbitrary mixture of helium and quencher may be specified with the appropriate density and atomic number for the quencher used. The span of cells required to contain the events under any given specification is self-adjusting.

No attempt is made to include the effects of the intrinsic pulse-height spread of the gas counter. For energy deposits in the region of interest to us (>100keV) the intrinsic counter spread is of the order of a few percent FWHM. The effect of this on the very wide and shapeless pulse height spectrum in a cell is negligible. Similarly, the effect of electron diffusion in the gas is neglected. This acts to spread the energy deposits among adjacent cells with a spatial standard deviation (σ) which is of the order of 0.5mm/$\sqrt{}$cm of drift at ambient pressure in the gas mixtures we are typically using. In most of the geometries under study this will have at most a marginal effect.

In its basic form the model is designed for detectors in the shape of independently instrumented parallel strips (i.e. one-dimensional readout); however, as will be shown below the results can be used to give a useful assessment of the performance of various forms of two-dimensional detectors.

3. COMPARISON OF THE MODEL WITH THE BEAM MONITOR DATA

The measured performance of the GMSD beam monitor reported in reference [1] is available as a test of the monte carlo model. The parameters of the detector (d=3mm, c=1.2mm, h=80mm, gas filling ^{3}He and CO_2) were inserted into the model which produced the spatial resolution curve shown in figure 1. The agreement of the shapes of the simulated and experimental (TEB14664) response curves is good . (A beam spread of 1mm has been included to simulate the 1mm slit collimator used in the experiment.) The main uncertainty in modelling the test GMSD is in the proportions of the gas mixture. The mixing system was very crude and the detector window leaked steadily so it is not surprising that the best simulation of the beam profile is obtained with a mixture of 20% helium to 80% CO_2 instead of the nominal 50% / 50% which was intended. The low helium fraction also tends to be confirmed by the low detection efficiency (0.14%) which we estimated in the practical test. The model gives 0.34% for our assumed mixture which is probably within the limits of agreement set by our poor estimates of the beam parameters.

As well as giving a plausible fit to the observed spatial resolution of the GMSD beam monitor, the model reproduces the general features observed in the experimental runs, namely the characteristic double distribution of the point-spread function (usually

fitted by a sum of two gaussian curves) and the increase of the spatial resolution and the decrease of sensitivity with increasing discriminator setting [1].

4. A HIGH RESOLUTION BEAM MONITOR

The results obtained in the tests described above [1] showed that with a (nominal) gas filling of 50%^{3}He and 50%CO_2 a collimated 1mm wide beam was imaged with a point-spread function which could be fitted by a double gaussian with principal component (82% of events) showing a σ of 0.55mm (figure 1). The GMSD used in the tests has a basic cell width of 0.3mm (four cells were bussed into one readout channel) and the question arises as to just what spatial resolution may be attainable with this hardware. The model has been used to explore the modifications (relatively easy to achieve) which may make substantially sub millimeter spatial resolution possible.

Figure 2a shows the effect of increasing the stopping power of the quencher. First CF_4 is substituted for CO_2 (curve A), then the fraction of CF_4 is increased to 90% (still maintaining ambient pressure) (curve B) and finally a window overpressure of one bar is allowed with 0.5 bar of ^{3}He and 1.5 bar of CF_4 (curve C). The relative amplitudes of the curves reflect the trigger efficiency, the detection efficiencies calculated are, A:0.8%, B:0.196%, C:1.2%. The point spread functions (PSF) show the usual double distributions. Gaussian fits to the main (narrower) distribution show that it is difficult to significantly decrease the width. The σ values (parameter b in the fits) are, A:0.535mm, B:0.433mm, C:0.356mm. The LLD value of 0.1MeV was chosen as optimum via preliminary runs with the LLD varied from 0.05 to 0.45MeV.

Unlike a wire counter, the GMSD can operate happily with a very narrow drift gap and in a beam monitor the loss of detection efficiency in a narrow gap is not a problem. Figure 2b compares the PSFs with helium and CF_4 (50/50) at ambient pressure as the counter depth (d) is reduced from 3 to 1mm. The results are not satisfactory; although a narrow gaussian appears which has (at d=1mm) σ = 0.0475mm, the fraction of events within it is very small (7.9%) and thus not very useful.

The model shows that to make a significant improvement in σ the drift gap must be narrowed ***and*** the pressure raised. Figure 2c shows the PSF when the gas is 0.5b ^{3}He + 1.5b CF_4 and d = 1mm. In this case 74.3% of the counts are in a gaussian with σ = 0.241mm. The estimated detection efficiency is 0.4%.

In this configuration diffusion is unlikely to contribute at this level and higher pressure may be able to push σ down to the 0.1mm level. At a spacing of 1mm the drift electrode is in the ideal position to form the pick-up electrode for the second dimension in a 2-d detector. The PSF in the second dimension should not be significantly worse than that calculated for the primary dimension.

5. AN IMAGING DETECTOR FOR *ENGIN*

The active area of the beam monitor GMSD reported in reference [1] is approximately 80mm x 80mm which, combined with a spatial resolution of around 1mm offers an attractive potential as an imaging detector for stressed engineering samples in the ENGIN facility on ISIS. In this case, however, a useful detection efficiency is a pre-requisite since good statistical quality is required.

The model has been used to explore the best options for modifying the detector to meet the requirements of ENGIN. Figure 3a shows the PSFs of a possible version as a function of the electronic threshold (LLD). The counter depth was set at d=3.0cm (since this is the maximum tolerable without compromising the neutron time-of-flight (TOF) resolution). The window over-pressure (3 bars absolute) has been restricted to two bars to avoid the containment becoming too complex. A 50/50 mixture of ^{3}He and CF_4 appears to give a good compromise between efficiency and spatial resolution. The cell (pixel) width is maintained at 1.2mm, as in the original tests. The data from the model runs shown in figure 3a are summarised in figure 3b. In this case the optimum LLD is around 0.35MeV giving a detection efficiency of 30% with a σ of 0.69mm. The multiplicity is 1.23 so the extra deadtime burden is quite small.

In order to image in the orthogonal dimension it is proposed to add a plane of wires spaced 1mm above the plate with a wire-to-wire spacing of 1mm. This should enable amplifiers connected to these wires to receive pulses of about 50% of the amplitude recorded in the strip anodes with very little extra spreading above that induced by the event tracks. Provided the noise level is kept down in the Y channel amplifiers it ought to be possible to keep the LLD at the same level as the anodes in MeV terms. Since one will require simultaneous triggers in both the X and Y channels for a valid event, the important parameter from the model is the trigger efficiency. If one assumes equivalent (in energy terms) LLDs in each channel then the efficiency for bi-dimensional readout is just the square of the trigger efficiency as measured by the model. In the present case with an LLD of 0.35MeV the trigger efficiency given by the model is 0.9865, giving a 2-d trigger efficiency of 0.973 , which is quite acceptable. Operating at LLD=0.38 gives a multiplicity of 1.0 (figure3b) and a trigger efficiency of 0.911 giving a 2-d trigger efficiency of 0.911^2 (=0.830) which is much the same as throwing away the 20% of double hits with the lower threshold.

In order to achieve 2-d imaging, in addition to the counter modifications, some modifications are required to the electronic systems. First, the existing front-end readout electronics must be duplicated; second, a facility for performing the X-Y coincidence must be provided; third, some form of interpolation and coding must be provided to sort out the multiple triggers to be expected in many events. (If the multiplicity can be kept as low as 20% then a simple option may be to reject multiple triggers.)

6. A GAS PIXEL DETECTOR FOR NEUTRON DIFFRACTION

For neutron diffraction studies it is desirable to have a detector which is capable of dealing with high localised rates. A pixel detector with its own dedicated readout is the ideal solution. Some time ago a gas pixel detector was developed at RAL for X-ray detection which had a pixel pitch of 0.1 inch (2.5mm) [3]. This scale matches well to the sample size generally used in neutron diffraction so the model has been used to evaluate the imaging performance of a neutron pixel detector based on this design.

The relatively large scale of the pixel means that the fraction of CF_4 required to contain the neutron events is not very high: a mixture of 1.5b ^3He + 0.5b CF_4 is proposed with a detector depth of d=3.0cm. Setting c=2.5mm, h=2.5mm in the model reproduces the response of a strip of pixels and so gives a cross-section of the 2-d pattern observed in the full detector. The efficiency and multiplicity measured in this way will both be low because event tracks which fail to trigger pixels in the row under study still may trigger pixels in adjacent rows. In order to better estimate the detection efficiency and the multiplicity the model was rerun with a large value of h to catch all events.

Figure 4a shows the PSF curves derived from the model for a range of LLD values. Clearly the pixel almost totally contains the event so the measured σ of 0.472mm at LLD=0.25MeV is about what one would expect. Figure 4b summarises the data derived from figure 4a and from runs with the h dimension large (80mm) (for the detection efficiency and the multiplicity). An LLD of 0.25MeV is about optimum with a detection efficiency of 45.4% predicted. It will be noted that in figure 4b σ increases at high LLD values. This is a general feature of the model and reflects the fact that in this case the particles are almost stopping in the central cell and the large energy deposits of the bragg peak are dumped in the adjacent cells giving an increased spread and (at very high thresholds) a bimodal distribution.

The window overpressure of 1 bar was chosen to minimise mechanical problems and keep the operating HT from getting too high. If one is prepared to cope with the problems of adding a few more bar of helium (no more quencher is needed) the efficiency can be driven up to the 60-70% mark.

Depending on the electronic readout system chosen, the multiple hits may or may not cause problems. A properly developed 2-d model will be required to explore this problem with the readout logic built in. Prima facie the basic response of the pixel detector looks very promising. The hope is to build a basically tiled system with individual tiles sealed and electronically self-contained.

7. PROPOSAL FOR A VERY HIGH PRESSURE GMSD

The model has been used to evaluate the imaging performance of a GMSD detector in which it is proposed to have a gas filling of 15.4b ^3He + 0.6b CF_4 with a 3.0cm conversion depth. In the model the cell width has been set at 1.2mm. Figure 5a shows the series of PSFs produced by a range of LLD settings and figure 5b summarises the

data. An optimum working point is clearly around LLD=0.25MeV where the detection efficiency is nearly unity (97.6%) and the spatial resolution is σ = 0.79mm. Using our form of readout the multiplicity is 1.6.

The imaging performance predicted by the model is good and will give an excellent overall performance if the elevated operating HT required for 16 bars pressure is supported by the plate.

8. CONCLUSIONS

The monte carlo model of the imaging performance of one dimensional gas detectors with discrete readout channels seems to deliver reliable and consistent results. In general it shows that it is possible to generate an acceptable trade-off between the detection efficiency and the spatial resolution in all the potential applications which have been examined. The main extension required is to model 2-d detectors with their readouts in enough detail to confirm the extrapolations of the 1-d results. Taking only a few seconds to perform a single PSF simulation (on a Pentium Pro200), the model is a flexible tool available for input to the detector design process.

REFERENCES

1. J E Bateman, N J Rhodes and R Stephenson, RAL-TR-97-021

2. J F Janni, (1982) Atomic Data and Nuclear Data Tables, 27, Nos 2-5

3. J E Bateman and J F Connolly, A gas pixel detector for X-ray imaging, Proceedings of the European Workshop on X-ray Detectors for Synchrotron Radiation Sources, Aussois, France, September 1991, p92.

FIGURE CAPTIONS

1. The experimental position resolution measured with the GMSD beam monitor imaging a 1mm slit beam of neutrons (TEB14664), compared with the simulated response of the detector to the same beam. The curves are normalised together in peak amplitude.

2a. The simulated PSF of the beam monitor GMSD as the fraction of CF_4 quencher is increased. The detector depth (d) is kept at 3mm (with 0.3mm wide counter strips) throughout. The gas mixtures are indicated on the graph. The standard deviation of the gaussian fits is the parameter “b” in the curve legends.

2b. In these simulations of the beam monitor the gas mixture is kept constant (0.5b ^3He + 0.5bCF_4) and the detector depth set at 3mm, 2mm and 1mm. The fits to the two latter cases consist of a sum of two gaussians.

2c. In this simulated PSF for the beam monitor is seen the effect of having a narrow counter gap (1mm) and a high gas pressure ($0.5b^3He + 1.5bCF_4$).

3a. The simulated PSFs obtained with different discriminator LLD values for the proposed ENGIN detector are presented. The curves of the gaussian fits are listed in the order of the corresponding LLD value.

3b. A summary of the essential performance parameters of the ENGIN detector as a function of the electronic discriminator threshold selected.

4a. The simulated PSFs of a row (diameter) of the 2-d response of the proposed pixel detector. The various curves represent the response with different discriminator LLDs.

4b. A summary of the essential performance parameters of the proposed pixel detector as a function of the electronic discriminator chosen.

5a. The simulated PSFs of a proposed very high pressure GMSD as a function of the electronic LLD selected. The gaussian fit is to the data for LLD = 0.25MeV.

5b. A summary of the essential performance parameters of the very high pressure GMSD proposal as a function of the electronic threshold imposed.

FIGURE 1

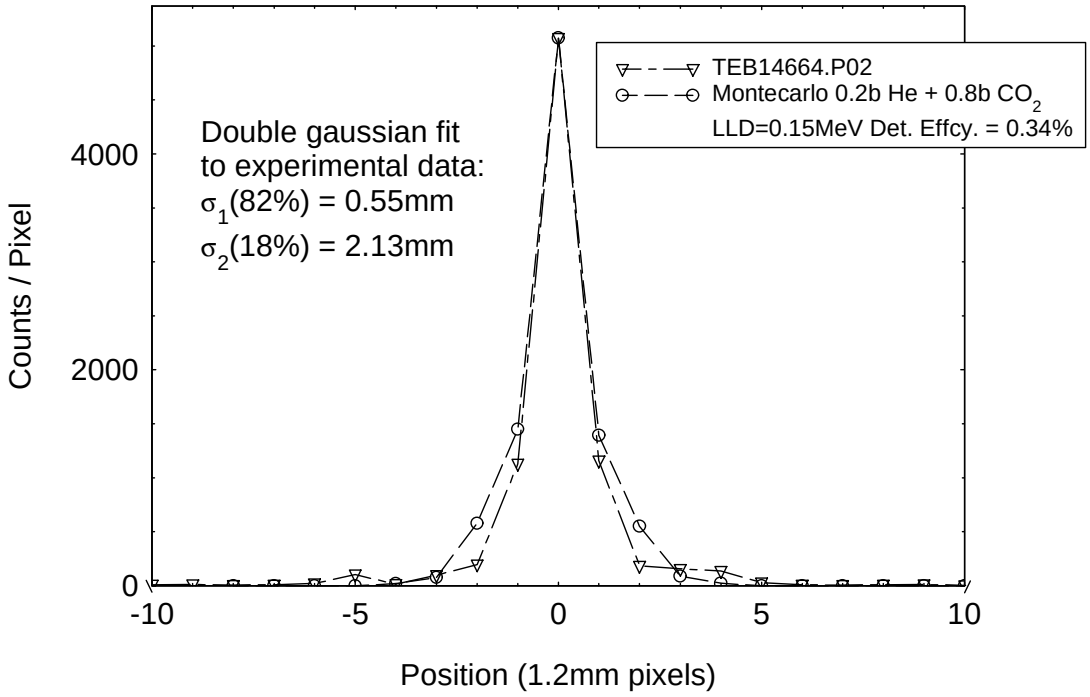

FIGURE 2a

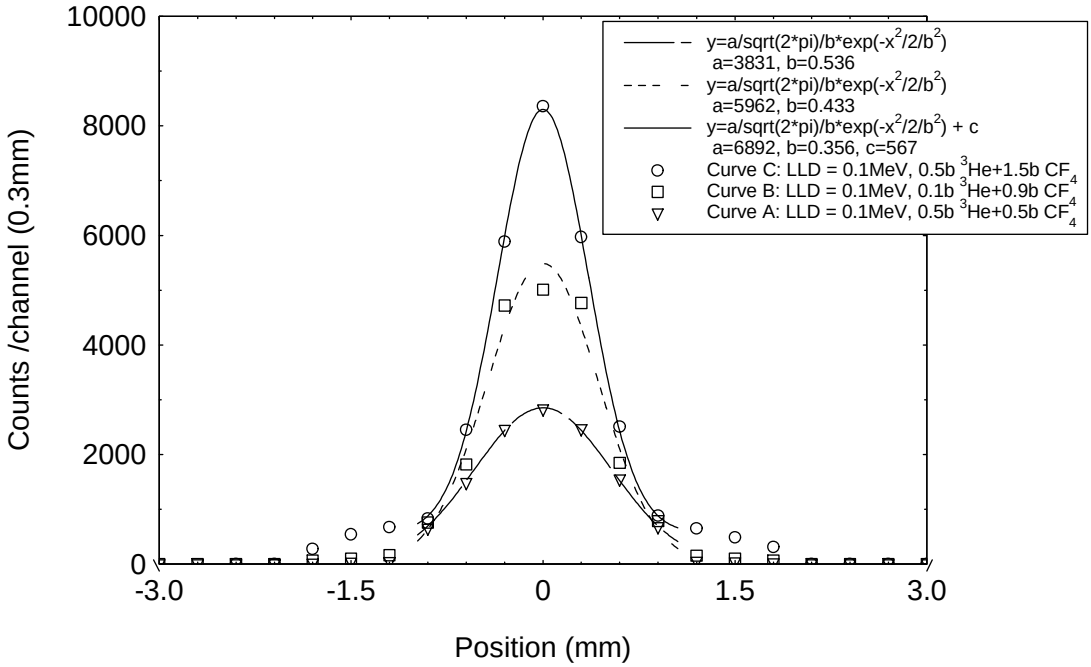

FIGURE 2b

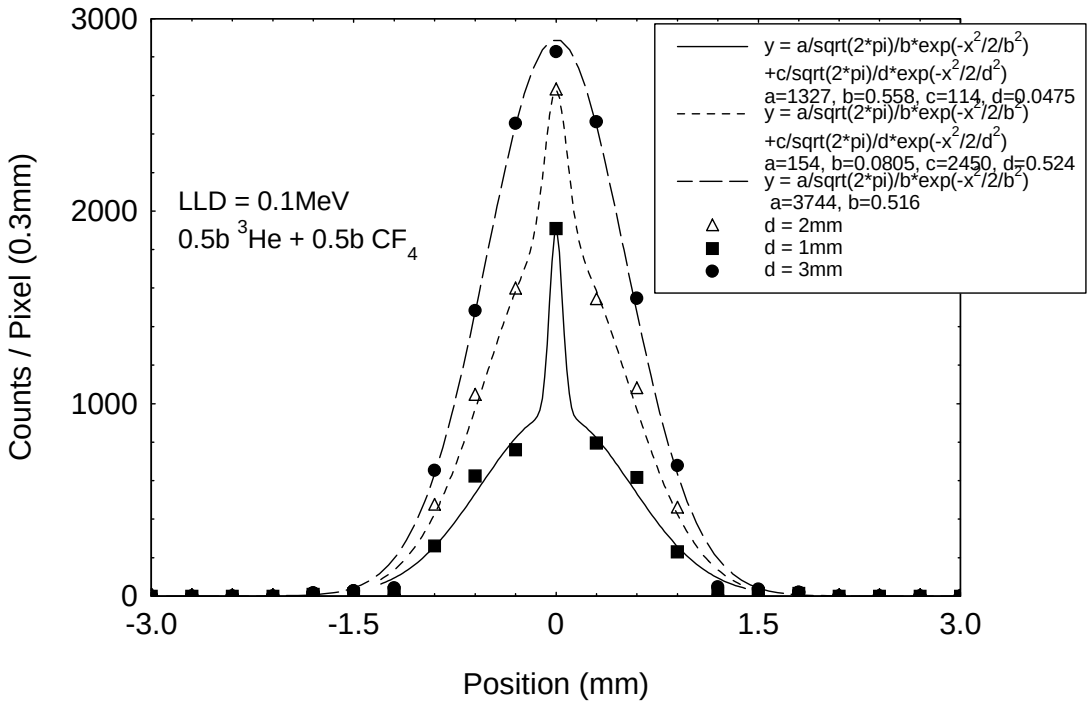

FIGURE 2c

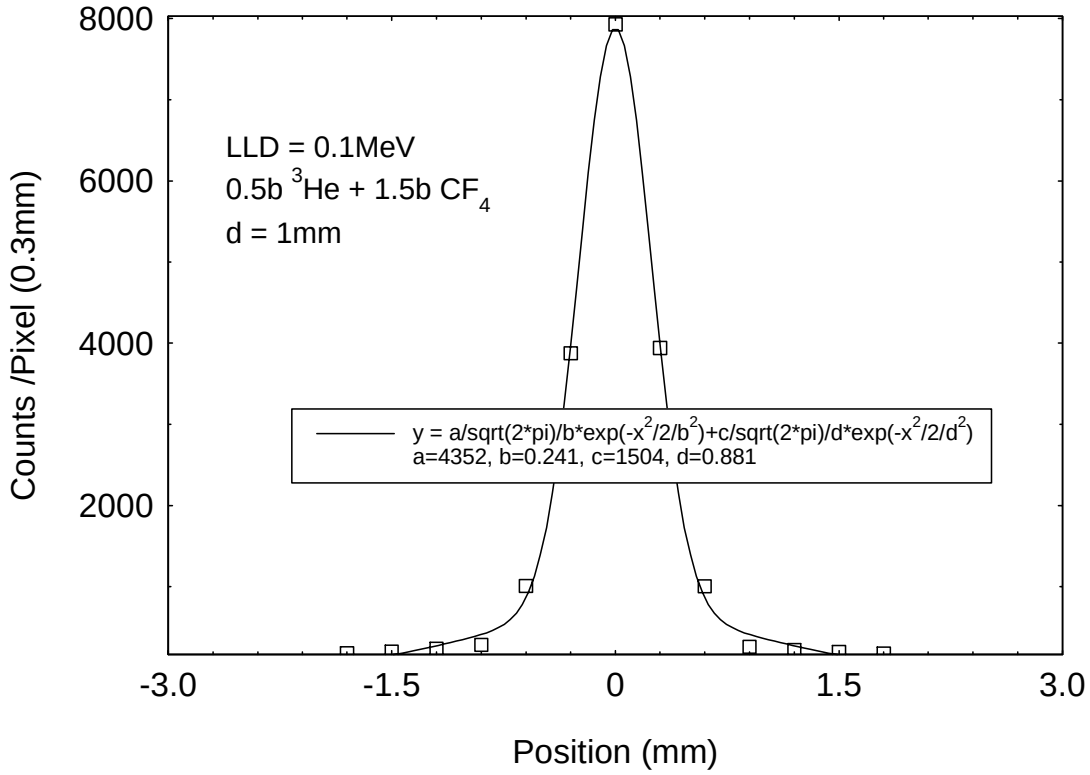

FIGURE 3a

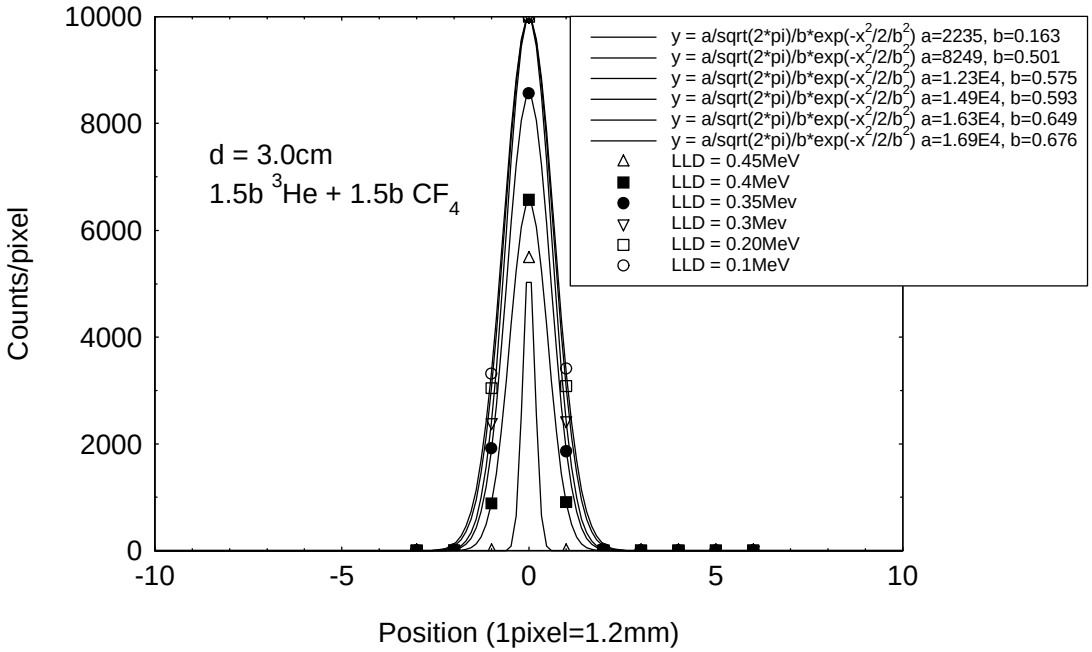

FIGURE 3b

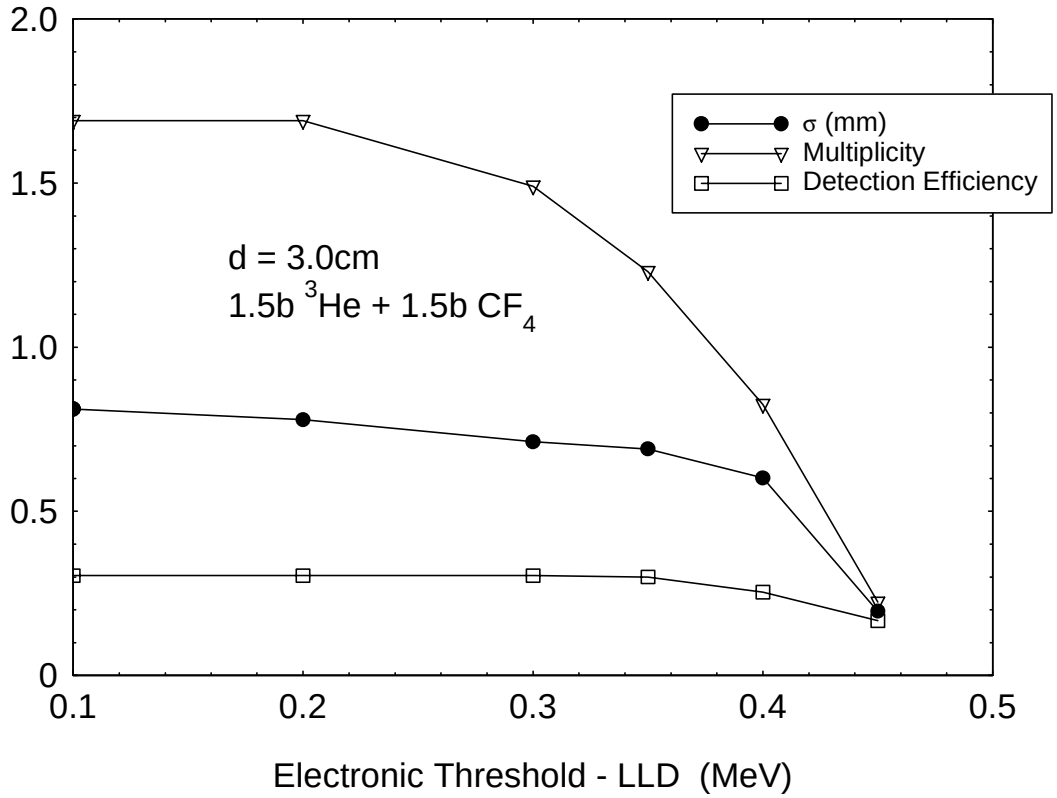

FIGURE 4a

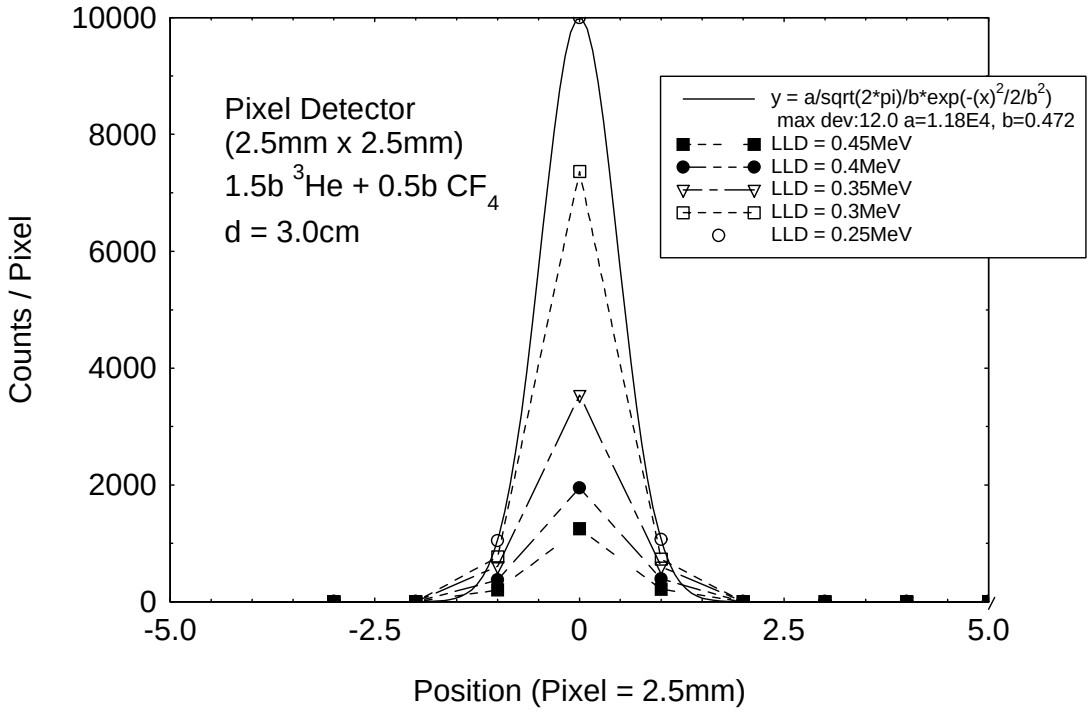

FIGURE 4b

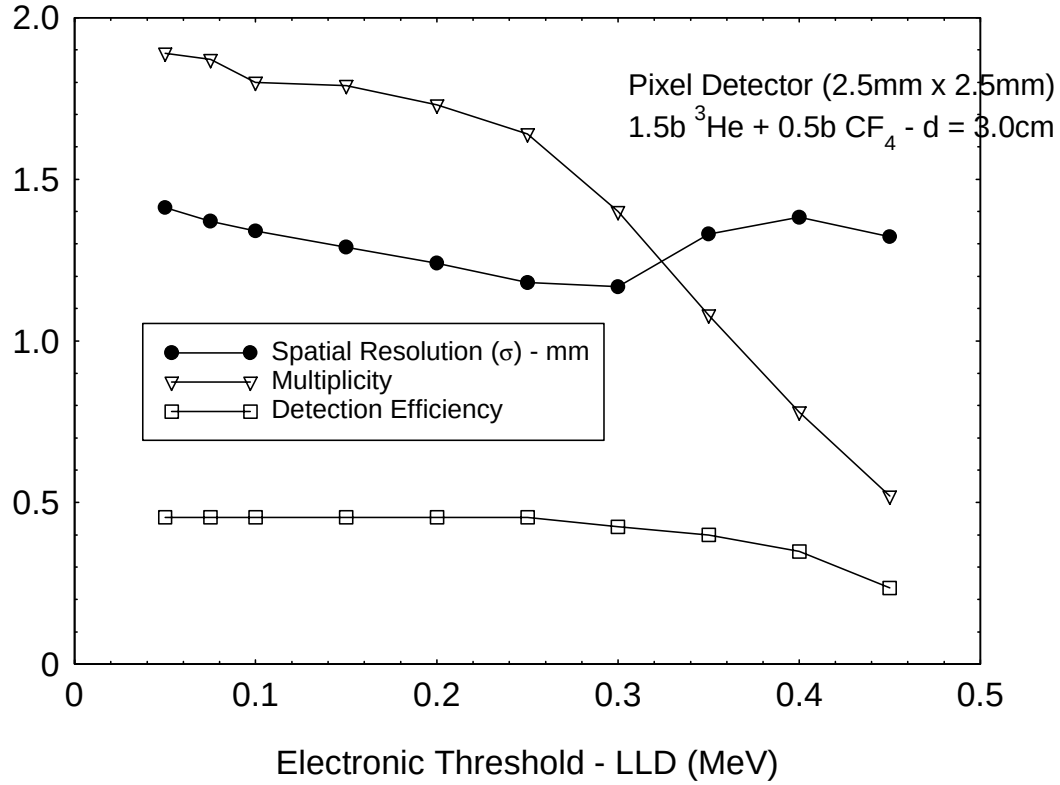

FIGURE 5a

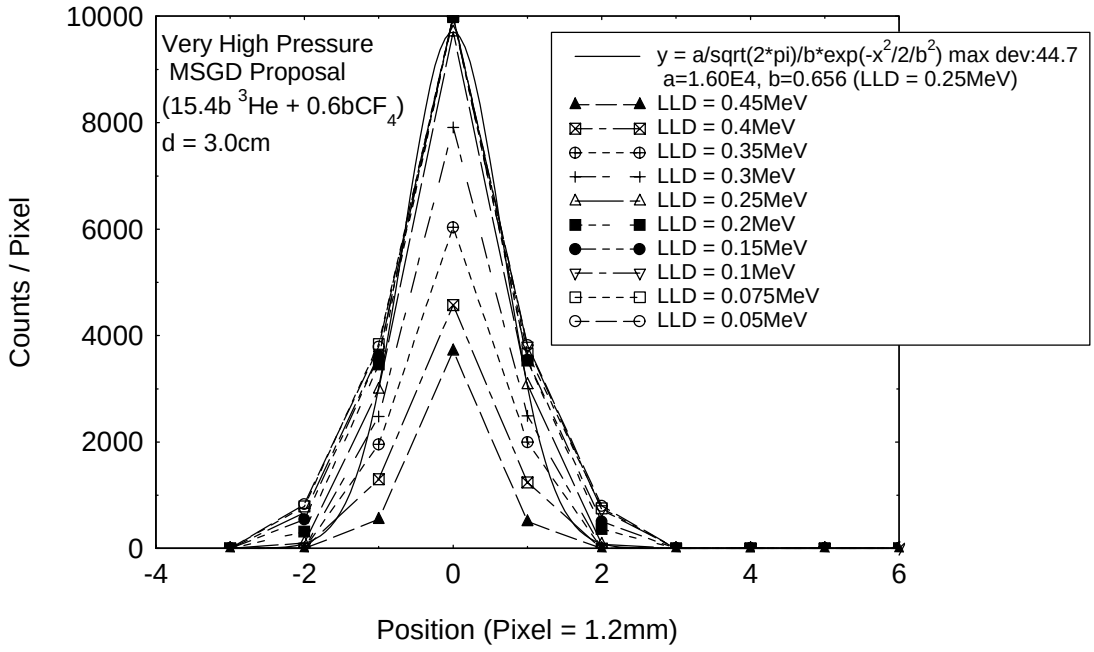

FIGURE 5b